Tightly Coupled Integration of Inertial Data with Multi-Constellation PPP-IF with Integer Ambiguity Resolution

D. Gallego Maya, R. Zaid, K. Y. Kouedjin, P. Sarri, A. Guinamard

SBG-Systems SAS - 1 avenue Eiffel - 78420 - Carrières-sur-Seine - France

KEY WORDS

PPP-IF-IAR, Tightly Coupled INS/GNSS, Integer Ambiguity Resolution, Multi-Constellation Fast Convergence.

ABSTRACT

Precise Point Positioning (PPP) is already the preferred technique for GNSS navigation; however, it suffers from a low convergence time that cannot be accepted for multiple applications. This paper expands on the state-of-the-art techniques to address this limitation and considerably decrease the convergence time. The developed algorithm consists of a tightly coupled implementation of inertial data with a multi constellation PPP Ionosphere-Free with Integer Ambiguity Resolution (PPP-IF-IAR). The first step to improve the convergence was to achieve the integer ambiguity resolution in a multi-constellation multi-frequency configuration. The addition of the inertial data proved to be essential in keeping a precise position during the GNSS signal disruptions commonly seen in land applications, moreover it ratified its importance by accelerating the ambiguity resolution. Another focus of this paper is the validation of the algorithm in real kinematic scenarios. The results will be presented as a series of two comparisons. Firstly, the solution will be compared to a Real Time Kinematic (RTK) very short base line reference solution. Secondly, the tightly coupled solution will be compared to the GNSS only PPP-IF-IAR solution.

I. INTRODUCTION

Since the early stages of the GNSS technology, the potential for precise geodetic positioning has been acknowledged by the research community. Multiple algorithms have been developed seeking a centimeter position accuracy. During the 90s, the vast majority of techniques focused on a relative positioning, where single and double differenced measurements were implemented to eliminate most of the GNSS measurement errors [1]. Zumberge et al. [2] introduced the PPP, a new technique that removed the need of a reference station. The observations equations, estimation models, and implementation details for PPP were described by Kouba et Héroux [3]. For the last 20 years, multiple articles have been published expanding on the concepts of the PPP algorithm. The ambiguity resolution of the carrier phase measurement was the main focus of the field, this research unlocked the full capacity of the phase observation and enhanced the position accuracy [4]. With the constant deployment of new satellites and constellations, the multi-constellation PPP with a greater availability was explored [5].

This paper will address the tightly coupled implementation of inertial data with a multi constellation PPP Ionosphere-Free with Integer Ambiguity Resolution (PPP-IF-IAR). An overview of the applied corrections will be discussed, from the precise satellite orbits and clock corrections to the satellite Phase Center Offsets and Variations (PCO/PCV) and phase wind-up estimation. Special attention was dedicated to the compatibility of the satellite products. The orbit and clocks of the Helmholtz Centre Potsdam GFZ German Research Centre for Geosciences (GFZ) [6] were used with the absolute satellite bias generated by the CNES. The well known Narrow-lane (NL) and Wide-lane (WL) scheme ([7], [8]) was used to fix the IF ambiguity as described by Pan et al. [9]. The integer ambiguity resolution was a crucial part of the development of the tightly coupled algorithm, it enhanced the PPP accuracy even further allowing a coupled solution with a new level of precision in kinematic mode. The developed algorithm benefits from a multi-constellation configuration. Exploring different frequency bands and signals channels was a challenging aspect of the implementation, but it proved to be essential in increasing the availability and robustness of the algorithm, that currently operates using GPS L1/L2/L5 and GALILEO E1/E5a/E5b/E6. The main drawback of PPP is its long convergence time. This subject was also explored and improved by the implementation of multiple combinations that can be used to generate an additional measurement considerably less noisy than the IF pseudo-range measurement ([10], [11]). In kinematic mode, the convergence time of the position solution was decreased considerably with the ambiguity resolution and the less noisy measurement combination.

Another main focus of this paper will be the validation of the tightly coupled INS/PPP-IF-IAR solution in kinematic mode. Until now, the assessment of PPP in kinematic mode consists of a series of static data-sets that are processed using a kinematic propagation model. We will present the performance of our algorithm in a series of real kinematic acquisitions, both in land and marine applications, and our results will be directly compared to a high performance RTK very short base line solution. A second comparison will be made between the tightly coupled INS/PPP-IF-IAR solution and a pure PPP-IF-IAR solution, this will provide a better understanding of the augmented integrity and robustness of a multi sensor integration.

II. MATHEMATICAL MODEL

PPP is rapidly replacing RTK as the de facto technique for GNSS positioning. However, it needs a careful modeling of local and environmental effects which is more challenging than the double differential approach. A crucial point in the adoption of the PPP was the availability of precise orbits and clock solution products that impulsed its research in many applications. The satellite orbits and clocks must be fixed, and the used PPP model should be consistent with the network solution model that was used to estimate those products.

The model used for this paper consists of a dual-frequency combination that allows us to eliminate the majority of the Ionosphere propagation delays. Equation (1) represents the basic mathematical model of the pseudorange and carrier phase observations while equation (2) shows the model for the second band. The Ionosphere-free combination (3) eliminates nearly all of the ionospheric propagation errors.

$$\begin{aligned} P^s_{r,1} &= \rho + c(dt_r - dt^s) + I^s_r + T^s_r + (d_{r,1} - d^s_1) + \epsilon_1 \\ \phi^s_{r,1} &= \rho + c(dt_r - dt^s) - I^s_r + T^s_r + (\delta_{r,1} - \delta^s_1) + \lambda_1 N^s_{r,1} + \lambda_1 \omega^s_r + \varepsilon_1 \end{aligned} \tag{1}$$

$$\begin{aligned} P^s_{r,2} &= \rho + c(dt_r - dt^s) + \alpha I^s_r + T^s_r + (d_{r,2} - d^s_2) + \epsilon_2 \\ \phi^s_{r,2} &= \rho + c(dt_r - dt^s) - I^s_r + T^s_r + (\delta_{r,2} - \delta^s_2) + \lambda_2 N^s_{r,2} + \lambda_2 \omega^s_r + \varepsilon_2 \end{aligned} \tag{2}$$

$$\begin{aligned} P^s_{r,IF} &= \rho + c(dt_r - dt^s) + T^s_r + (d_{r,IF} - d^s_{IF}) + \epsilon_{IF} \\ \phi^s_{r,IF} &= \rho + c(dt_r - dt^s) + T^s_r + (\delta_{r,IF} - \delta^s_{IF}) + \lambda_{IF} N_{IF} + \lambda_{IF} \omega^s_r + \epsilon_{IF} \end{aligned} \tag{3}$$

Where:

- $P^s_{r,IF}$ is the ionosphere-free combination of two pseudorange observations in two different frequencies.
- $\phi^s_{r,IF}$ is the ionosphere-free combination of two carrier phase observations in two different frequencies.
- ρ is the geometrical range.
- dt_r is the receiver clock offset.
- dt^s is the satellite clock offset.
- c is the vacuum speed of light.
- T^s_r is the troposphere delay.
- ($d_{r,IF}$, d^s_i) are the code signal specific range biases related to the transmitter and receiver.
- ($\delta_{r,IF}$, δ^s_i) are the phase signal specific range biases related to the transmitter and receiver.
- N_{IF} is the non-integer ambiguity of the IF carrier phase combination.
- λ_{IF} is the IF combination of the carrier phase wavelength.
- ω^s_r is the phase wind-up effect.
- ϵ_{IF} measurement noise of the IF combinations.

As the satellite orbits and clocks are considered fixed for the model, the unknown parameters of equation (3) are the receiver position, the receiver clock offset, the troposphere delay and the non-integer IF carrier phase ambiguity. Furthermore, a single difference approach using a reference satellite for each system can simplify the model by eliminating the receiver dependent parameters.

III. PPP CORRECTIONS

At a user level, the basic observation models (1 and 2) must be corrected in order to eliminate some of the most considerable effects that disturb the GNSS signals. When working with pure pseudorange observations, only the larger errors tend to be corrected to achieve a meter level precision. However, using the precise satellite products and the dual frequency combination implies that even the more subtle effects must be accounted for. The more common corrections include the relativistic effects ([12], [13]), the atmospheric effects ([14], [15], [16]), the satellite clock offset, signal biases, multi-path, etc. Most of these corrections are well known and considered a standard for GNSS navigation, therefore a more detailed description will be omitted from this article.

In this section, a summary of the more delicate corrections will be presented, they are normally neglected in typical implementations, but for the PPP case they must be carefully considered.

Carrier Phase Wind-Up

Opposite to the pseudorange measurements, the carrier phase not only changes as a function of the distance between the transmitter and the receiver, but also with the attitude of both antennas relative to the line of sight vector. This effect is known as phase wind up, and even though it can be comfortably ignored in differential positioning algorithms with a short base line, it impacts the performance of the PPP and must be considered.

It should be mentioned that for mobile applications, the rotation of the receiver antenna about its fixed axis (yaw) results in an equal wind-up effect for all tracked satellites. The more delicate aspect of the phase wind-up corrections arrives from the satellite attitude maneuvering, specially during noon and midnight turns in the eclipse season where the attitude changes are most pronounced.

The phase wind-up cannot be overlooked, as it is typically considered by the analysis centers that generate the satellite products. As a result, neglecting the phase wind-up while fixing the satellite orbits and clocks in the PPP model can generate a decimeter error in the estimated position. The wind-up effect can be calculated following the guidelines of the IGS products ([17]).

Phase Center Offsets and Variations

Contrary to the broadcast ephemeris, the precise products refer to the satellite's center of mass instead of the antenna phase center. As the GNSS measurement refer directly to the phase center, it is of crucial importance to compensate such offset between the measurement and the satellite's reference point. Even though this is the most important factor to account for when considering the antennas, as it translates to a couple of meters of error if not properly corrected, other corrections must be applied in order to unlock the centimeter level precision. Similarly to the phase center offset (PCO) of the satellites, the receiver antenna also suffers from this phenomenon, accounting for the offset between the receiver's reference point and the antenna phase center eliminates a decimeter level error. Finally, the phase center variations (PCV), which depend of the azimuth and elevation angles, represent a smaller portion of the budget error with a few mm, but nevertheless they must be corrected.

The aforementioned PCO and PCV values for satellites and receivers are distributed and regularly updated by the IGS in a standard format called Antenna Exchange Format (ANTEX) [18]. More detailed information about the calibration of this values can be found in the works of Rothacher & Mader [19] and Schmid et al. [20].

Additional Corrections

The full description of all the other corrections is out of the scope of this paper, more details about the different effects that affect the GNSS signals and the models to correct them are discussed by Steigenberger [21] and Kouba & Lahaye [22]. A summary of the whole error budget and compensations that needs to be achieved is described in the Table 1 (adapted from Kouba & Lahaye [22]):

Model component		Magnitude
Satellite	Antenna PCO	≈ 1.5 m
	Antenna PCV	≈ 10 mm
	Satellite bias	≈ 1 m
	Clock offset	≈ 1 ms
	Relativistic clock	≈ 10 m
Atmosphere	Troposphere (dry)	≈ 2.3 m
	Troposphere (wet)	≈ 0.3 m
	Ionosphere (1er order)	≈ 30 m
	Ionosphere (higher order)	≈ 2 cm
Site Displacement	Plate motion	≈ 0.1 m/y
	Solid Earth Tide	≈ 0.4 m
	Ocean loading (tidal)	≈ 5 cm
	Ocean loading (non tidal)	≈ 10 mm
	Pole tide	≈ 25 mm
	Atmospheric loading (tidal)	≈ 1.5 mm
	Atmospheric loading (non-tidal)	≈ 20 mm
Receiver	PCO	≈ 10 cm
	PCV	≈ 3 cm
	Receiver bias	≈ 1 m
Others	Phase wind-up	≈ 10 cm

Table 1: Approximate PPP correction models. Adapted from [22]

IV. INTEGER AMBIGUITY RESOLUTION

PPP with integer ambiguity resolution has been one of the most important research topics in recent years. It can enhance the performance of the algorithm by not only improving the precision of the estimated solution, but also by reducing the convergence time. The ambiguity resolution is very challenging for the PPP approach, mainly because nearly all the effects that impact the GNSS measurements must be corrected or eliminated [9].

The non-integer ambiguity of the IF combination from (3) can be defined as a combination of the Wide-Lane ambiguity and the Narrow-Lane ambiguity (4), both having an integer value. The float WL ambiguity can be estimated using the Melbourne-Wübenna combination and it can be easily fixed by rounding methods once it has converged thanks to its long wavelength.

$$N_{IF} = \frac{f_1 f_2}{f_1^2 - f_2^2} N_{WL} + \frac{f_1}{f_1 + f_2} N_1 \tag{4}$$

Equation (5) shows the float NL ambiguity derived from Equation (4). Now, the traditional Mlambda method (Equation 6) can be used to fix these ambiguities. The covariance matrix used as an input of Mlambda is expressed in 7, with $P_{N_{IF}}$ being the covariance of the IF ambiguity in the estimation filter, and $P_{N_{WL}}$ being zero assuming that the WL ambiguity was successfully fixed.

$$N_1 = \frac{f_1 + f_2}{f_1} N_{IF} - \frac{f_2}{f_1 - f_2} N_{WL} \tag{5}$$

$$\left[\check{N}_1, res, P_s\right] = mlambda(N_1, P_{N_1}) \tag{6}$$

$$P_{N_1} = \left(\frac{f_1 + f_2}{f_1}\right)^2 P_{N_{IF}} + \left(\frac{f_2}{f_1 - f_2}\right)^2 P_{N_{WL}} \tag{7}$$

V. TIGHTLY COUPLED INTEGRATION

For the tightly coupled (TC) integration, the GNSS navigation processor is neglected in order to directly use the pseudorange and carrier phase measurements as inputs for the Extended Kalman Filter [23]. The sensor fusion between the INS and GNSS data is performed in the range domain. This architecture is more challenging than the loosely coupled integration, but it improves the performance of the navigation solution and gives extra advantages such as the individual characterization of each satellite measurement, allowing a fault detection and exclusion before it affects the final solution. Figure (1) shows the TC architecture used in this algorithm.

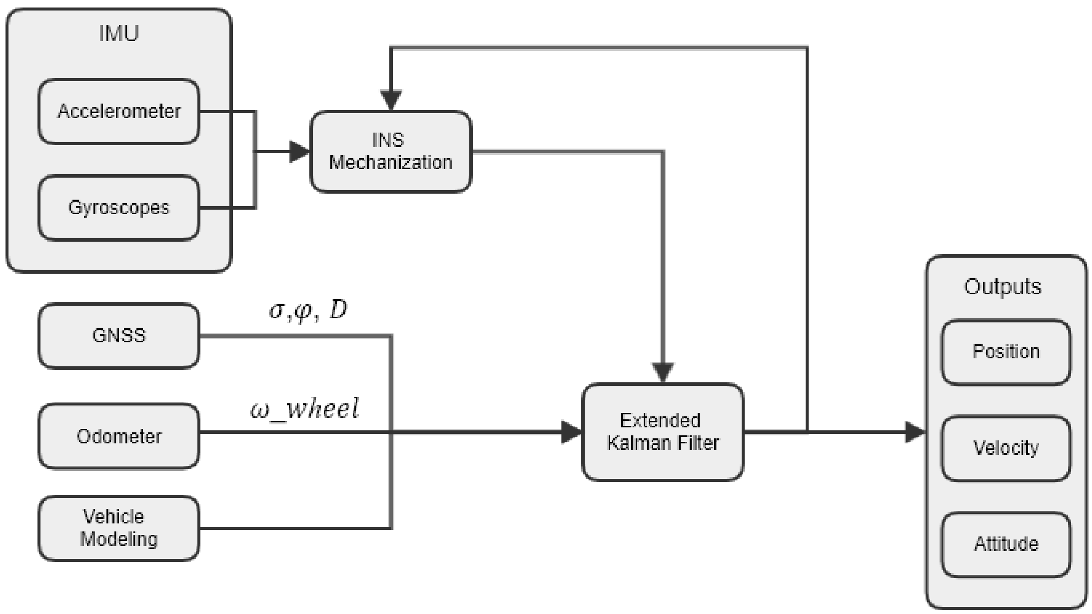

Figure 1: Tightly Coupled INS/GNSS Integration Architecture.

VI. TESTS AND RESULTS

Many articles have already validated the performance of PPP algorithm in static applications. In terms of precision, it has matched the performance of RTK, and despite its longer convergence time, considerable improvements have been made in recent years. In this article we take a step forward to analyze the performance of the PPP in real kinematic applications, focusing on the convergence time in both GNSS only and INS/GNSS tightly coupled integration.

The performance analysis will focus on two main applications, automotive and marine. For all the following test a kinematic reference will be calculated using an RTK short base line algorithm. The convergence time will be evaluated as the time it takes to reach a sub 10 cm horizontal error. For each test, multiple full resets of the estimation filter will be applied in order to create multiple convergence periods and therefore have meaningful statistics for the analysis.

1. Automotive

The automotive scenario consists of an open sky environment in a countryside area near Paris, France. The base station SBGS was used in the generation of the reference trajectory using an RTK short base line algorithm. Three different devices were used during this test, a GNSS receiver, a MEMS IMU and a FOG IMU. These devices allow three different system configurations, a GNSS only mode, a tightly coupled INS/GNSS using the MEMS IMU and a tightly coupled using the FOG IMU. The trajectory for this test can be seen in Figure 2.

Figure 2: Qinertia Overview of Automotive Test Trajectory

Navsight Ekinox

Navsight Land/Air Ekinox (Figure 3) consists of an Ekinox IMU connected to a robust processing unit embedding data fusion, and for our test, a Septentrio GNSS receiver. This solution has been designed to bring simplicity and versatility in a cost-effective package for testing and surveying applications. It achieves up to 0.02 deg. of Roll and Pitch precision in RTK mode, up to 0.05 deg. in GNSS-based heading in a short baseline configuration and offers an easy odometer connection plus a post-processing capability with Qinertia PPK software.

Figure 3: Navsight Ekinox.

a) GNSS PPP IF AR

Figure 4 shows the horizontal error obtained using the PPP GNSS only algorithm. After convergence, a 2 - 3 cm precision is kept during the whole duration of the log. Figure 5 gives a closer look at the convergence time for this test. From a cold start the solution reaches a sub 10 cm error in the 2D position after 256 seconds.

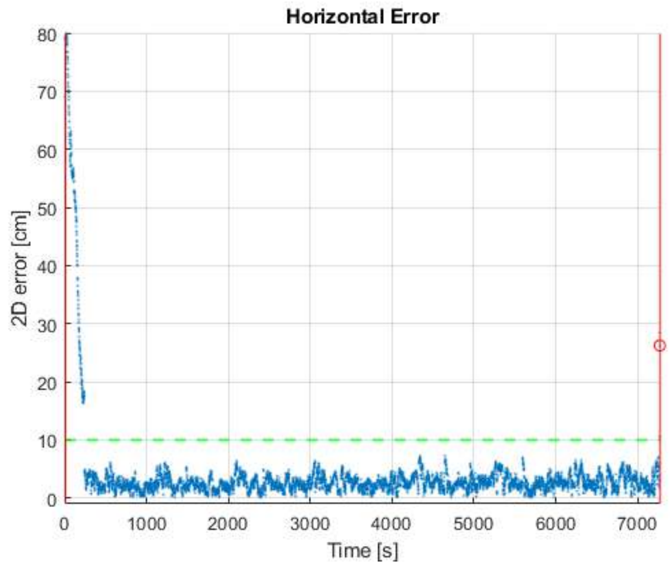

Figure 4: GNSS Only PPP-IF-IAR: Navsight Ekinox Results in Kinematic Mode.

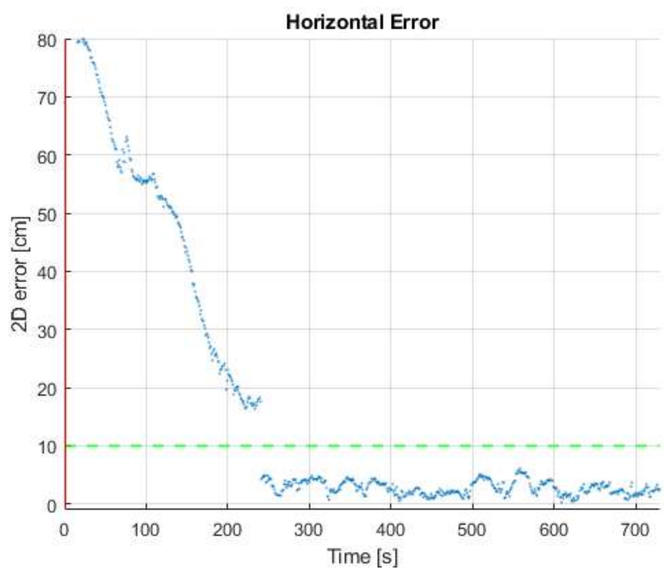

Figure 5: GNSS Only PPP-IF-IAR: Navsight Ekinox Zoomed Results in Kinematic Mode.

A more in depth analysis of the convergence time can be accomplished by resetting the system multiple times during the test. In our case, the Extended Kalman filter was fully reset every 5 minutes. By doing this, not only the estimated integer ambiguities of the carrier phase measurements are rebooted, but also the atmospheric and inertial states will need to be re-estimated. The impact of the resets can be seen clearly in the 2D error position (Figure 6), where every 5 minutes the error increases considerably but it then rapidly regains the expected precision. Figure 7 resumes the convergence time after each reset, the average convergence time for this test is 128 seconds, which is already very impressing for a PPP GNSS only configuration in a real kinematic mode.

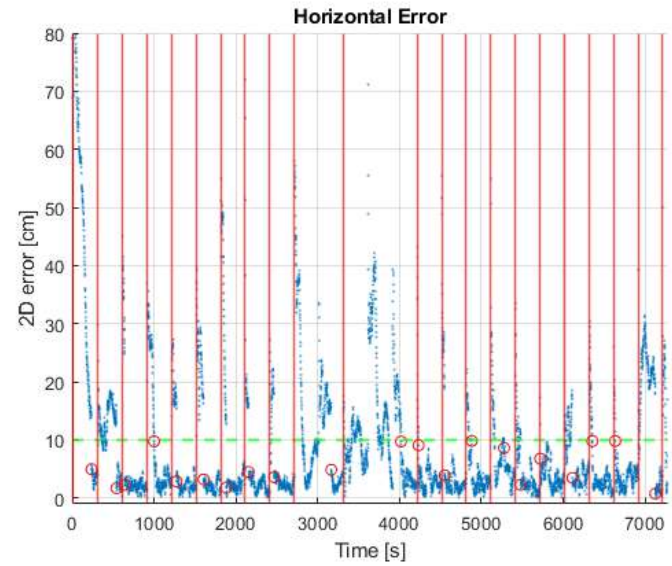

Figure 6: GNSS Only PPP-IF-IAR: Navsight Ekinox Horizontal Error.

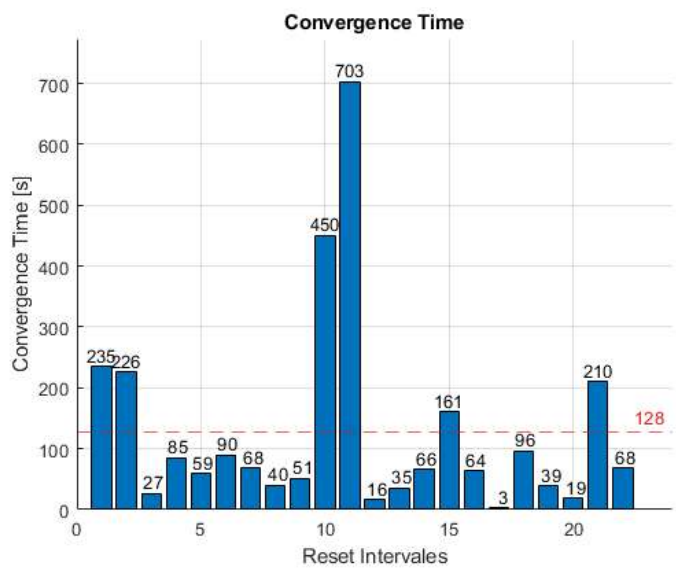

Figure 7: GNSS Only PPP-IF-IAR: Navsight Ekinox Convergence Time.

b) Tightly Coupled MEMS IMU/GNSS PPP IF AR

To analyse the convergence time of the tightly coupled solution, the system was reset every 5 minutes by forcing it into an AHRS mode. After every reset, the time needed to regain a sub 10 cm solution was quantified. Figure 8 illustrates the horizontal error after the AHRS resets while Figure 9 summarizes the convergence time of every period. In this case, the average convergence time is 66 seconds, more than 50 % faster than in the GNSS only mode.

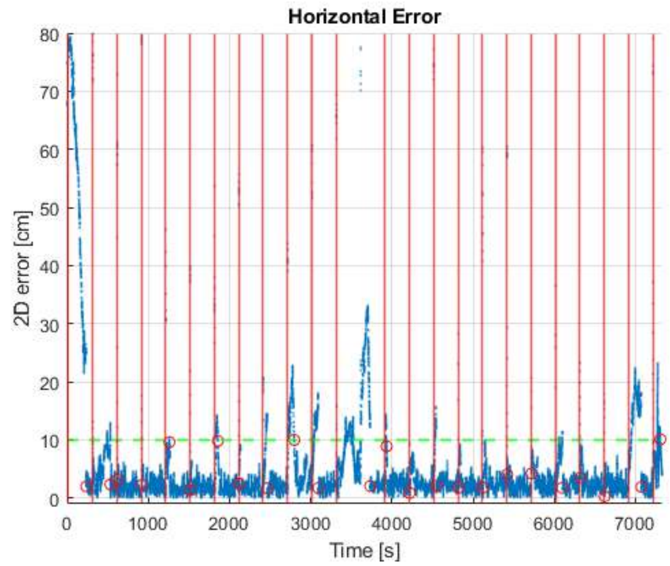

Figure 8: Tightly Coupled INS/GNSS PPP-IF-IAR: Navsight Ekinox Ambiguity AHRS Resets Horizontal Error.

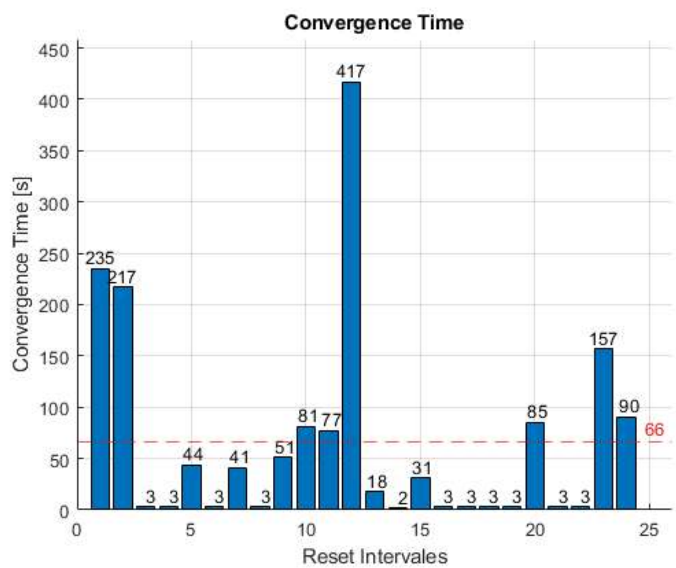

Figure 9: Tightly Coupled INS/GNSS PPP-IF-IAR: Navsight Ekinox Ambiguity AHRS Resets Convergence Time.

The improvements of the tightly coupled integration over the GNSS only mode during this test are substantial. A mean convergence time of slightly more than a minute in an automotive application can open new doors for PPP in the navigation field. It can be considered that the gain of performance comes from the coupled architecture regardless of the technology of the INS sensor. The following configuration will provide the information for a direct comparison between the GNSS/MEMS and the GNSS/FOG implementations.

Navsight Horizon

Horizon IMU brings Navsight (Figure 10) to the most demanding environments such as high altitude surveying, highly dense areas, and applications where only a single antenna can be used. Horizon IMU is based on a closed-loop FOG technology which enables ultra-low bias and noise levels. It allows robust and consistent performance even in a low dynamics survey. It provides up to 0.007 deg. of Roll and Pitch precision in RTK mode, up to 0.01 deg. in GNSS-based heading (single antenna) in a short baseline configuration and also offers an easy odometer connection and a post-processing capability with Qinertia PPK software.

Figure 10: Navsight Horizon.

c) Tightly Coupled FOG IMU/GNSS PPP IF IAR

It is important to note that between the previous configuration and this one, only the INS sensor has been changed. The results presented below were obtained using the same GNSS receiver but this time it was coupled with a FOG IMU.

The tightly coupled configuration demonstrated once again that the INS addition to the system guarantees a higher level of robustness compared to the GNSS only solution. Figure 11 displays the horizontal error of the tingly coupled solution after the filter is reset several times into an AHRS mode. The average mean time was reduced from 128 seconds to 62 seconds. A synthesis of the convergence time of this solution is presented in Figure 12. The results from the two tightly coupled solutions are very similar, using the FOG IMU only provides a slight improvement over the MEMS configuration. The data obtained during this experimentation suggests that the INS enhances the convergence time of the PPP algorithm regardless of the technology of the sensor.

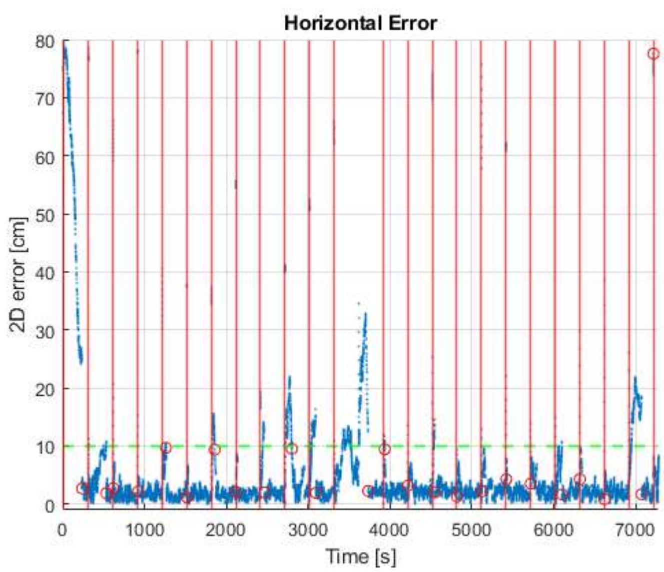

Figure 11: Tightly Coupled INS/GNSS PPP-IF-IAR: Navsight Horizon Ambiguity AHRS Resets Horizontal Error.

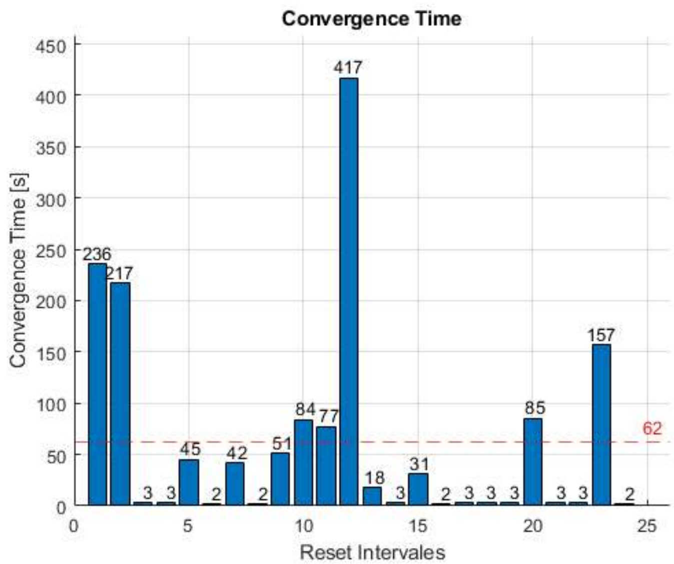

Figure 12: Tightly Coupled INS/GNSS PPP-IF-IAR: Navsight Horizon Ambiguity AHRS Resets Convergence Time.

2. Marine

Another interesting application of the PPP algorithm is for offshore applications were the differential methods such as RTK may lack the availability of a base station. The following test was conducted in the coast of Brazil, using a Navsight Apogee Sub-Sea system coupled with a Septentrio GNSS receiver in a survey mission. The trajectory of this test is illustrated in Figure 13.

Figure 13: Qinertia Overview of Marine Test Trajectory

Navsight Apogee Marine

Highly versatile, Navsight Apogee grade delivers the best performance under GNSS outages, making it ideal for challenging shallow to deep-water applications (Figure 14). Its performance goes up to 0.008 deg. in Roll and Pitch, 0.015 deg. heading (GNSS-based), 1 cm RTK GNSS position, 5 cm heave, 2 cm delayed heave, making it the ideal solution for all hydro-graphic tasks.

Figure 14: Navsight Apogee Marine.

a) GNSS PPP IF AR

Firstly, the precision of the GNSS only solution is validated using an RTK short baseline reference. Figure 15 displays the horizontal error, after the initial convergence the error is consistently kept under the sub 10 cm limit. From a cold start, the position converges after just a couple of seconds.

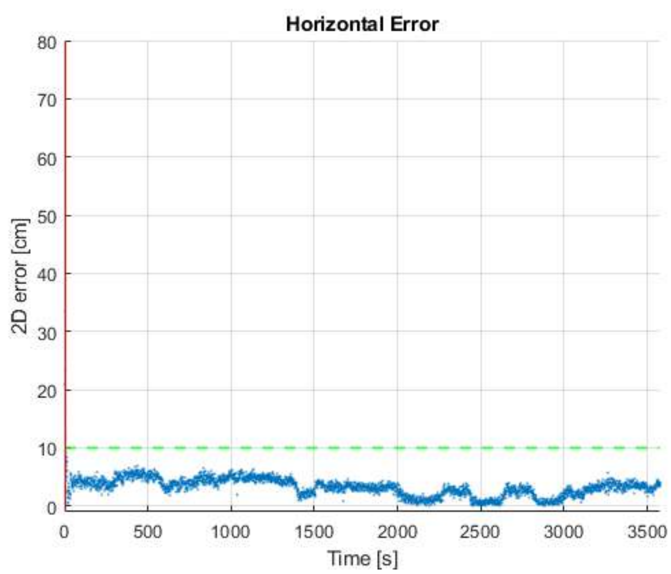

Figure 15: GNSS Only PPP-IF-IAR: Navsight Marine Results in Kinematic Mode.

The same strategy as before is used in this marine test. Every 5 minutes the system was reset to create multiple periods of convergence and analyze the behavior of the algorithm. This particular test in shorter than the two previous, so less periods are available for the analysis. Figure 16 shows how the 2D error convergences to a sub 10 cm mark after every reset. Figure 17 illustrates more clearly the convergence time of each period, on average the filter converges to the target precision after 26 seconds.

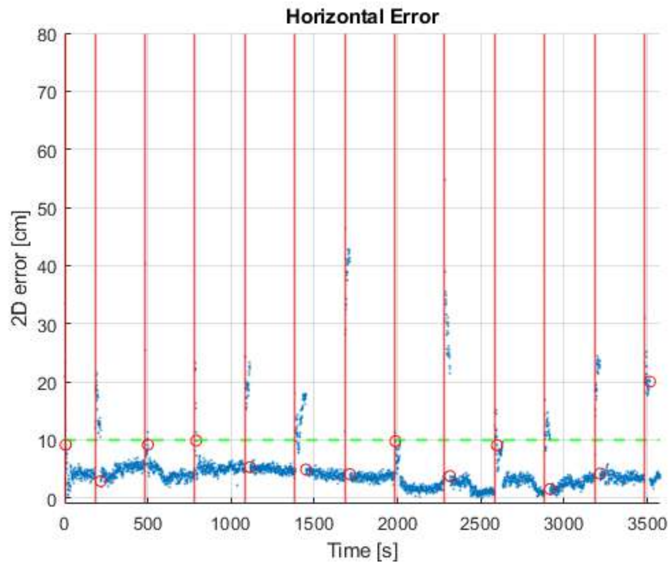

Figure 16: GNSS Only PPP-IF-IAR: Navsight Marine Horizontal Error.

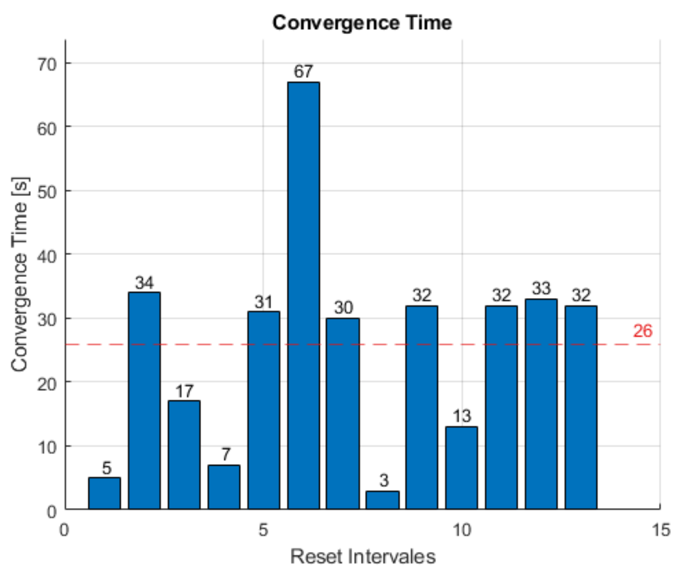

Figure 17: GNSS Only PPP-IF-IAR: Navsight Marine Convergence Time.

b) Tightly Coupled INS/GNSS PPP IF AR

The average convergence time for this test was already excellent in GNSS only mode, however the tightly coupled configuration continues to improve the performance of the PPP. It can be seen in Figure 18 that the horizontal error convergences almost instantly below the target limit just a couple of seconds after every reset. Figure 19 highlights that the average convergence time is only 10 seconds, which can be considered a new standard for PPP in marine applications.

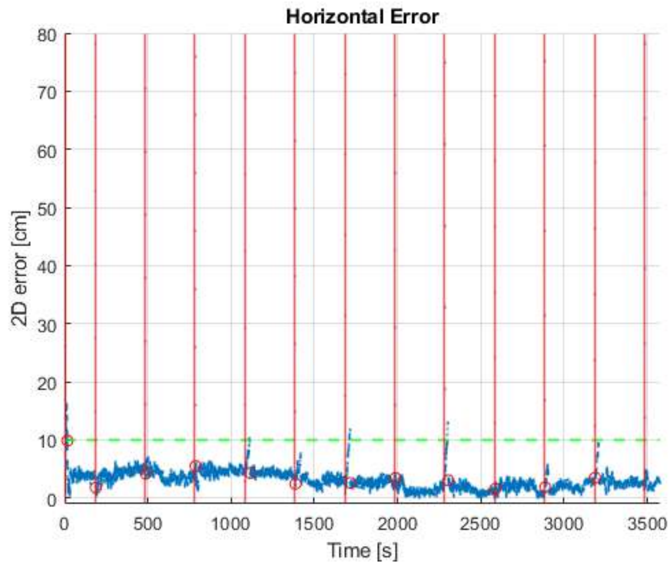

Figure 18: Tightly Coupled INS/GNSS PPP-IF-IAR: Navsight Marine Ambiguity AHRS Resets Horizontal Error.

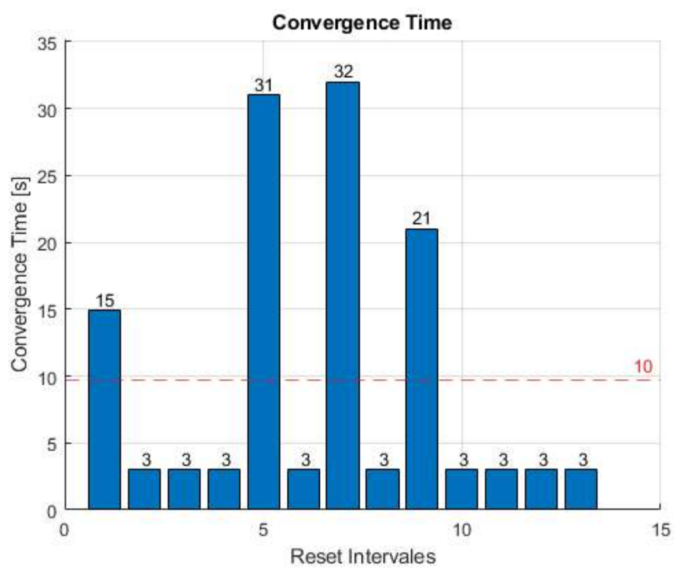

Figure 19: Tightly Coupled INS/GNSS PPP-IF-IAR: Navsight Marine Ambiguity AHRS Resets Convergence Time.

The open sky environment and the slow dynamics of a survey boat can be considered as the ideal conditions for PPP. Therefore, the convergence time in this application is significantly faster than in the automotive case. Despite this, a constant is seen in both scenarios as the tightly coupled integration improves upon the GNSS only results with a big impact on the convergence time.

3. Summary

The results for both applications in all the tested configurations are summarized in Table 2. The GNSS only results are outstanding on their own, a convergence time of just a couple of minutes in kinematic applications are now a reality for the PPP. Even more, the tightly coupled results reach new levels of convergence, settling the new standard for the PPP algorithm.

	Automotive			Marine	
	GNSS	Tightly Coupled MEMS	Tightly Coupled FOG	GNSS	Tightly Coupled
Mean Convergence Time	128 s	66 s	62 s	26 s	10 s

Table 2: Results Summary

VII. CONCLUSIONS

The implemented algorithm settles the new standards for PPP. This has been proved with real kinematic data where the convergence of the position solution is more challenging. Significant improvements over the state of the art methods have been made essentially by coupling the GNSS receiver with an inertial sensor in a tightly coupled architecture. The tested configurations proved that the benefit from the INS is meaningful regardless of the technology of the sensor. The results obtained unlock a handful of new applications for the GNSS positioning, as the fast convergence PPP is now a reality.

REFERENCES

[1] S. Verhagen, “The GNSS integer ambiguities: Estimation and validation,” 01 2005.

[2] J. Zumberge, M. Heflin, D. Jefferson, M. Watkins, and F. Webb, “Precise point positioning for the efficient and robust analysis of gps data from large networks,” *Journal of Geophysical Research*, vol. 102, 04 1997.

[3] J. Kouba and P. Héroux, “Precise point positioning using IGS orbit and clock products,” *GPS Solutions*, vol. 5, pp. 12–28, 10 2001.

[4] D. Laurichesse, F. Mercier, J.-P. Berthias, P. Broca, and L. Cerri, “Integer ambiguity resolution on undifferenced GPS phase measurements and its application to PPP and satellite precise orbit determination,” *Navigation*, vol. 56, pp. 135–149, 06 2009.

[5] K. Yang, H. Chai, B. Dong, Y. Zhou, D. Li, and P. Zongpeng, *BDS Zero-Difference Zero-Combination Precise Point Positioning Algorithm Study*, 01 2016, pp. 493–501.

[6] M. Uhlemann, G. Gendt, M. Ramatschi, and Z. Deng, *GFZ Global Multi-GNSS Network and Data Processing Results*, 01 2015.

[7] W. Melbourne, “The case for ranging in GPS-based geodetic systems,” *Proceedings of the First International Symposium on Precise Positioning with the Global Positioning System*, pp. 373–386, 01 1985.

[8] G. Wübbena, “Software developments for geodetic positioning with GPS using TI 4100 code and carrier measurements,” *Proceedings of 1st International Symposium on Precise Positioning with the Global Positioning System*, pp. 403–412, 01 1985.

[9] L. Pan, C. Cai, R. Santerre, and Z. Jian-Jun, “Combined GPS/GLONASS precise point positioning with fixed GPS ambiguities,” *Sensors (Basel, Switzerland)*, vol. 14, pp. 17 530–17 547, 09 2014.

[10] D. Laurichesse. (2015) Handling the biases for improved triple-frequency PPP convergence. [Online]. Available: https://www.gpsworld.com/innovation-carrier-phase-ambiguity-resolution/

[11] D. Laurichesse and S. Banville. (2018) Innovation: Instantaneous centimeter-level multi-frequency precise point positioning. [Online]. Available: https://www.gpsworld.com/innovation-instantaneous-centimeter-level-multi-frequency-precise-point-positioning/

[12] S. Zhu and E. Groten, “Relativistic effects in GPS,” *Lecture Notes in Earth Sciences, Berlin Springer Verlag*, 01 1988.

[13] Z. Hecimovic, “Relativistic effects on satellite navigation,” *Tehnicki vjesnik/Technical Gazette*, vol. 20, pp. 195–203, 02 2013.

[14] J. Klobuchar, “Ionospheric effects on GPS,” *Global Positioning System: Theory and Applications*, vol. 1, 01 1996.

[15] J. Saastamoinen, “Atmospheric correction for the troposphere and the stratosphere in radio ranging satellites,” *Geophys. Monogr. Ser.*, vol. 15, 01 1972.

[16] J. Marini, “Correction of satellite tracking data for an arbitrary tropospheric profile,” *Radio Science*, vol. 7, 03 1972.

[17] J. Kouba, “A guide to using international GNSS service (IGS) products,” 04 2009.

[18] M. Rothacher and R. Schmid. (2010) ANTEX: The antenna exchange format, version 1.4. [Online]. Available: https://files.igs.org/pub/data/format/antex14.txt

[19] M. Rothacher and G. Mader, “Receiver and satellite antenna phase center offssets and variations,” *Proceedings of the Network, Data and Analysis Centre 2002 Workshop, Ottawa*, pp. 141–152, 2002.

[20] R. Schmid, G. Mader, and T. Herring, “From relative to absolute antenna phase center corrections,” *Proceedings of the IGS Workshop and Symposium 2004, Bern*, 2005.

[21] P. Steigenberger, “Accuracy of current and future satellite navigation systems,” Ph.D. dissertation, Technische Universitat Munchen, 03 2017.

[22] T. P. Kouba J., Lahaye F., *Springer Handbook of Global Navigation Satellite Systems - Precise Point Positioning*, 1st ed., ser. 2522-8692. Springer International Publishing, 2017, ch. 25, pp. 723–752.

[23] P. Groves, *Principles of GNSS, Inertial, and Multisensor Integrated Navigation Systems, Second Edition*, 03 2013.